HHS Public Access

Author manuscript

Ophthalmic Genet. Author manuscript; available in PMC 2016 January 09.

Published in final edited form as:

Ophthalmic Genet. 2016 March ; 37(1): 44–52. doi:10.3109/13816810.2014.929716.

Ocular Phenotype of a Family with FAM161A-associated Retinal Degeneration

Jacque L. Duncan[1], **Pooja Biswas**[2], **Igor Kozak**[2], **Mili Navani**[2], **Reema Syed**[1], **Shiri Soudry**[1], **Moreno Menghini**[1], **Rafael C. Caruso**[3,4], **Brett G. Jeffrey**[3], **John R. Heckenlively**[5], **G. Bhanuprakash Reddy**[6], **Pauline Lee**[2,7], **Austin Roorda**[8], and **Radha Ayyagari**[2]

[1]Department of Ophthalmology, University of California, San Francisco, CA, USA

[2]Shiley Eye Center, University of California, San Diego, La Jolla, CA, USA

[3]National Eye Institute, NIH, Bethesda, MD, USA

[4]Princeton Neuroscience Institute, Princeton University, Princeton, NJ, USA

[5]Department of Ophthalmology, University of Michigan, Ann Arbor, MI, USA

[6]National Institute of Nutrition, Indian Council of Medical Research, Hyderabad, India

[7]Department of Molecular and Experimental Medicine, The Scripps Research Institute, La Jolla, CA, USA

[8]School of Optometry and Vision Science Graduate Group, University of California, Berkeley, CA, USA

Abstract

Background—Characterization of retinal degeneration (RD) using high-resolution retinal imaging and exome sequencing may identify phenotypic features that correspond with specific genetic defects.

Materials and Methods—Six members from a non-consanguineous Indian family (three affected siblings, their asymptomatic parents and an asymptomatic child) were characterized clinically, using visual acuity, perimetry, full-field electroretinography (ERG), optical coherence tomography and cone structure as outcome measures. Cone photoreceptors were imaged in the proband using adaptive optics scanning laser ophthalmoscopy. The exome was captured using Nimblegen SeqCap EZ V3.0 probes and sequenced using lllumina HiSeq. Reads were mapped to reference hg19. Confirmation of variants and segregation analysis was performed using dideoxy sequencing.

Results—Analysis of exome variants using exomeSuite identified five homozygous variants in four genes known to be associated with RD. Further analysis revealed a homozygous nonsense mutation, c.1105 C>T, p.Arg335Ter, in the *FAM161A* gene segregating with RD. Three additional

Correspondence: Radha Ayyagari, PhD, Shiley Eye Center, Jacobs Retina Center, Rm 206, University of California San Diego, 9415 Campus Point Drive, San Diego, CA 92093, USA. Tel: +1 858 534 9029. rayyagari@ucsd.edu.

DECLARATION OF INTEREST

Austin Roorda holds patents on AOSLO technology (US Patents #7,118,216 and 6,890,076) and he is a consultant on AOSLO technology to Canon, Inc. There are no other conflicts of interest to report.

variants were found to occur at high frequency. Affected members showed a range of disease severity beginning at different ages, but all developed severe visual field and outer retinal loss.

Conclusions—Exome analysis revealed a nonsense homozygous mutation in *FAM161A* segregating with RD with severe vision loss and a range of disease onset and progression. Loss of outer retinal structures demonstrated with high-resolution retinal imaging suggests *FAM161A* is important for normal photoreceptor structure and survival. Exome sequencing may identify causative genetic variants in autosomal recessive RD families when other genetic test strategies fail to identify a mutation.

Keywords

Exome sequencing; *FAM161A*; retinal degeneration

INTRODUCTION

Recessive mutations contribute to a significant proportion of cases with retinal degeneration (RD). Mutations in more than 140 genes have been identified in patients with recessive RD (RetNet webpage accessed March 8, 2014 from https://sph.uth.tmc.edu/Retnet/sum-dis.htm). The large number of genes, heterogeneity and significant overlap in the phenotype of various RDs, and lack of information describing unique clinical features associated with particular disease genes complicate the molecular and clinical diagnosis and necessitate the screening of all genes associated with RD phenotypes. Recent advances in clinical imaging provide an opportunity to understand the specific cellular components of the retina involved in pathology and progression of degeneration. If distinct clinical features that characterize particular genetic mutations can be identified, the search to identify the genetic mutation associated with autosomal recessive RD may be refined. In addition, exome sequencing has been established as a valuable tool for efficient screening of all genes known to be associated with retinal degenerations.[1,2] Precise characterization of the phenotype and genotype of retinal dystrophy patients and families using advanced clinical imaging and next generation sequencing methodologies will enable targeted genetic testing based on particular phenotypic features that have been observed in families with specific mutations.

Homozygosity mapping of a large consanguineous Indian family with a form of autosomal recessive retinal degeneration (arRD) identified the RP28 locus on chromosome 2p11-p15.[3] Mutations in the *FAM161A* gene have been reported as the underlying cause of retinal degeneration in families mapping to the RP28 locus. All *FAM161A* mutations reported in RD patients to date are either nonsense or frameshift mutations implicating functional loss of this gene in retinal pathology.[4–6] Phenotypes associated with *FAM161A* mutations include the development of early symptoms of night blindness, myopia, fundus characteristics typical of retinitis pigmentosa (RP), constricted visual fields and reduced ERG responses.[3–7] However, patients have shown a wide range of disease onset and severity with visual acuity ranging from 1.0 to light perception, optic disc pallor, limited bone spicule pigmentation, OCT thinning with relative preservation at the fovea, and severely reduced full-field ERG responses with cone flicker amplitudes significantly lower than among patients with other forms of arRP.[4] Some affected individuals also showed atrophic macular degeneration or a tapetal macular reflex, features not typical of RP.[3,7] These reports

demonstrate that mutations in *FAM161A* result in a variable phenotype possibly influenced by environmental or genetic modifiers.[4,5]

The present study describes exome analysis of an affected member of a non-consanguineous Indian pedigree with three siblings affected with recessive RD and identification of a homozygous nonsense sequence variant in the *FAM161A* gene segregating with the disease. These patients underwent detailed clinical evaluation using high-resolution retinal imaging techniques, including spectral domain optical coherence tomography (SD-OCT) in all three affected siblings, and adaptive optics scanning laser ophthalmoscopy (AOSLO) in the proband. The studies provide insight into how *FAM161A* mutations affect retinal structure in humans, and the potential role of *FAM161A* in preserving photoreceptor structure and viability.

MATERIALS AND METHODS

Research procedures were performed in accordance with the Declaration of Helsinki. The study protocol was approved by the University of California, San Francisco and University of California, San Diego institutional review boards. All individuals provided written informed consent before participating in the study, and the subjects who underwent high-resolution retinal imaging received a stipend. A two-generation family of Indian descent with one affected female and two affected male siblings (Figure 1) was studied. The oldest sister died at the age of 23 from a fever and was not believed to have had retinal degeneration. Both parents (II-1 and II-2) provided blood samples for genetic analysis. There was no known consanguinity, but both parents were from the Nadar caste in the Tamil Nadu region of India where, until recently, marriages were typically arranged within the caste.

Genetic Analysis

Prior genetic testing in III-1 revealed no mutations in *rhodopsin, peripherin/RDS, CRX, CRB1*, and in III-2 had revealed no mutations in the *RPGR* and *RP2* genes. DNA was isolated from blood samples collected from the parents and all three living, affected siblings. The exome of patient III-2 was captured using Nimblegen SeqCap EZ V3.0 probes and sequenced using Ilumina HiSeq. Sequence reads were mapped to reference hg19, and variants were called using standard protocols (Edge Bio, Gaithersburg, MD). All variants including nucleotide substitutions, insertions and deletions were filtered using exomeSuite; variants present in genes known to be associated with retinal degeneration were identified.[8] Variants located in known RD genes or predicted to be novel and potentially pathogenic were further evaluated by PCR and dideoxy sequencing for segregation analysis.

Clinical Examination

A complete history was obtained and records dating to 1991 were reviewed for the affected family members. Best-corrected visual acuity (BCVA) was measured using a standard chart according to the Early Treatment of Diabetic Retinopathy Study (ETDRS) protocol. Goldmann kinetic perimetry was performed using target sizes ranging between V-4e and I-1e.

Pupils were dilated with 1% tropicamide and 2.5% phenylephrine prior to obtaining color fundus photographs using a digital Topcon 50EX camera (Topcon Medical Systems, Oakland, NJ). Time-domain OCT images were acquired in 2005 on III-1 when the subject used central fixation (Stratus Fast Macular protocol, Carl Zeiss Meditec AG); SD-OCT images were obtained in subjects III-2 and III-3 as described previously,[9] and fundus autofluorescence (FAF) images (Spectralis HRA + OCT Laser Scanning Camera, Heidelberg Engineering, Vista, CA) were acquired in all affected family members after focusing the retinal image in the infrared reflection mode at 870nm by adjusting the sensitivity at 488nm and acquiring nine single 30 by 30 degrees FAF images through the macula and part of the optic disc. A barrier filter at 500nm suppressed the blue argon excitation light so that reflectance signals did not contribute to the FAF image.

Full-field electroretinography (ERG) was performed after 40 minutes of dark adaptation using Burian-Allen contact lens electrodes (Hansen Ophthalmic Development Laboratory, Iowa City, IA), according to the International Society for Clinical Electrophysiology and Vision (ISCEV) standards[10] and as described elsewhere.[11]

AOSLO Image Acquisition and Cone Spacing Analysis

High-resolution images were obtained using AOSLO in each eye of subject III-2 at age 39, and images were analyzed using custom-written software to determine cone spacing measures using previously described methods.[11,12] Cone spacing measures were compared with measures from 24 age-similar control subjects and z-scores, standard deviations from the mean value of control subjects, were reported; z-scores greater than 2 were considered abnormal.

RESULTS

Genetic Analysis

Sequencing the exome of III-2 and analysis of variants using exomeSuite identified five homozygous nucleotide substitutions in four genes: *PDE6B* (rs10902758), *DFNB31* (rs6478078), *BBS2* (rs4784677) and two homozygous mutations in *FAM161A*. One of the mutations in *FAM161A* encoded a homozygous nonsense change in exon 3, c. 1105 C>T, p.Arg335Ter (NM_001201543.1), which has been previously reported in patients with retinal degeneration.[6] In addition, a second mutation encoded a rare, homozygous, probably damaging (PolyPhen score = 0.999) change in exon 6, c.1791 G>T, p.Glu597Asp (rs201052209). Variants detected in the *PDE6B*, *DFNB31* and *BBS2* genes were reported to occur at high frequency in various populations (http://www.ncbi.nlm.nih.gov/SNP). Segregation analysis of the homozygous c.1105 C>T, p.Arg335Ter change and the rare homozygous c.1791 G>T, p. Glu597Asp change in the *FAM161A* gene established segregation of these two variants with RD in this pedigree (Figure 1). These changes were detected in the heterozygous state in the asymptomatic parents demonstrating that both mutations were located on the same allele (in cis). Neither mutation was detected in 100 unrelated controls from southern India.

Clinical Evaluation

Review of the clinical and family history revealed autosomal recessive inheritance of retinal degeneration in three offspring of Indian parents. There was no known consanguinity, but both parents were members of the Nadar caste of South India (Figure 1). We studied six members of this pedigree spanning three generations including the three siblings (III-1, III-2 and III-3) affected with severe RD but who were otherwise healthy. The children of III-1 were not examined but had no visual problems or complaints by their parents' report. The daughter of III-3, IV-1, was examined with visual acuity, kinetic perimetry, and optical coherence tomography and was normal with visual acuity of 20/16 and full visual fields to Goldmann perimetry in each eye.

Ophthalmic Evaluation

Clinical findings at the time of retinal degeneration diagnosis are summarized in Table 1. Family members with RD showed a range of disease severity and onset. The oldest two siblings developed loss of peripheral vision in their late teens, followed by difficulty with dark adaptation, nyctalopia and sensitivity to light in their 20s, visual acuity loss in their 30s, and severe loss of visual acuity (light perception in III-1 by age 40; and 20/200 in III-2, declining to light perception by age 42). The youngest sibling was evaluated at age 29 when he had no visual symptoms at the time his siblings were diagnosed (Table 1 and Figure 3); he developed difficulty with night vision beginning at age 42 and retained visual acuity of 20/40 in the right eye and 20/50 + 2 in the left eye at age 43. The three affected family members (III-1, III-2 and III-3) showed a bull's eye pattern of retinal pigment epithelial (RPE) atrophy in the macula, optic nerve head pallor and retinal vascular attenuation (Figure 2A–C). RPE mottling with grayish spots extended from the arcades to the periphery in III-1 which correlated with spots of hypofluorescence (Figure 2D), consistent with the RPE mottling described by Bandah-Rozenfeld and colleagues in other *FAM161A* RD patients.[4] Prominent bone spicule pigmentary change was present in III-2 (Figure 2B). Similar to other reported cases of *FAM161A* RD,[4] a ring of hyperfluorescence was observed in FAF images of the macula surrounding the fovea in all three patients, with central hypoautofluorescence in the two older siblings with advanced vision loss (Figure 2D–F). OCT images were obtained as close as possible to the anatomic fovea; in III-1, SD-OCT images were not obtained due to unstable fixation but time-domain OCTs were obtained at age 40 when fixation was stable and central. In all affected family members, OCT showed thinning and loss of the outer nuclear, inner segment (IS) and outer segment (OS) layers involving the fovea (Figure 2G–I). SD-OCT in III-2 showed hyper-reflective deposits in the outer retinal or subretinal space 2–3 degrees from the anatomic fovea (Figure 2, white arrows). The outer retinal layers were relatively preserved in the area surrounding the anatomic fovea in the youngest sibling (Figure 2I), similar to a previous report of subjects with *FAM161A* mutations and preserved visual acuity.[4]

Visual fields at diagnosis showed peripheral temporal scotomas with inferonasal crescents and severe constriction with small central islands in the oldest two siblings (Figure 3A and B). Visual fields were first evaluated in III-3 at age 29 while he was asymptomatic and showed midperipheral temporal scotomas to a I4e target (Figure 3C). Full-field ERG rod-mediated and cone-mediated responses were severely reduced below levels that can be

reliably measured in subjects III-1 and III-2 at diagnosis. Prior to the onset of any visual symptoms in III-3 at the time his siblings were diagnosed with retinal degeneration, full-field scotopic ERG amplitudes were reduced approximately 60% below normal, while cone-mediated responses were more severely affected with amplitudes reduced by 82% and 73% for the photopic single flash and 30Hz ERG responses, respectively. The implicit times of the cone-mediated responses were also delayed, consistent with widespread cone dysfunction (Figure 4).

AOSLO images were acquired from III-2 at age 39, when visual acuity was 20/100 and foveal sensitivity was 20 dB in each eye. SD-OCT showed severe loss of outer retinal layers throughout the macula with hyper-reflective profiles in the subretinal space at the fovea (Figures 5C and 6B). AOSLO images revealed diffuse atrophy and reflective profiles consistent with sparse residual cones (Figure 6A). Where cone mosaics were observed permitting quantitative analysis, cone spacing was increased by 6.9–8.9 standard deviations above the normal mean (Figure 6A1 and A2). Hyper-reflective profiles were observed in the outer retinal layers beneath the fovea and peripheral to the locations where cones were seen (Figure 6B). Although the youngest sibling, III-3, retained visual acuity of 20/40 OD and 20/50 + 2 OS, high-resolution images of retinal cones were not obtained using AOSLO, likely due to the patient's highly myopic refractive error.

DISCUSSION

Exome analysis of a single affected member of a recessive RD pedigree led to the identification of a homozygous nonsense change in the *FAM161A* gene segregating with the disease. Previously, *FAM161A* mutations have been implicated in causing arRD in Indian, German, and Palestinian families with a wide range of disease severity. The c.1105 C>T variant is located in exon 3 of *FAM161A* and alters arginine at position 335 to a stop codon (CGA>TGA) (NM_001201543.1). This change is predicted to cause premature truncation of the protein resulting in the loss of the C-terminal amino acids of the *FAM161A* protein, and has been reported in a Palestinian family with arRD.[6] This nonsense mutation may also lead to nonsense-mediated decay of the transcript resulting in complete loss of the protein. The second homozygous variant in exon 6, c.1791 G>T, p.Glu 597 Asp (rs201052209), is predicted to be damaging by PolyPhen (score = 0.999). If the nonsense mutation in exon 3 results in either premature truncation or leads to nonsense-mediated decay of the protein, the second c.1791 G>T may not have additional damaging effects on FAM161A. Identification of the nonsense mutation in the current Indian pedigree with arRD supports the hypothesis that loss of functional *FAM161A* leads to retinal degeneration involving both rods and cones.[3–7]

The function of *FAM161A* is not understood. However, *FAM161A* is evolutionarily conserved in vertebrates and highly expressed in developing and adult retina. Recent work indicates that *FAM161A* plays a role in microtubule stabilization by maintaining transport processes in photoreceptors as a component of the cilia-basal body complex along with cilia proteins lebercilin, CEP290, OFD1 and SDCCAG8.[13,14]

Consistent with previous reports of patients with *FAM161A* mutations,[3–7] the affected members of the current pedigree developed retinal degeneration affecting both rods and cones with early symptoms of nyctalopia and peripheral visual field loss, but they retained a central island of vision until advanced stages of disease. The current family also demonstrated variability in the onset and severity of retinal degeneration. The two oldest siblings followed a similar course with onset of nyctalopia in the second decade and vision loss progressing to light perception by the fifth decade. The youngest sibling, III-3, had a milder phenotype with symptom onset 10–13 years later than his siblings, although the pattern of visual field constriction was similar to III-1 and III-2. A recent report of a Palestinian family with the Arg335Ter mutation in *FAM161A* also demonstrated significant inter-individual variation in disease severity,[6] as was observed in the current study.

Bandah-Rozenfeld presented ERG findings on 28 affected members with *FAM161A* mutations and as in other reports, the majority of patients had extinguished ERG responses.[4] However, among three patients with recordable ERG responses, cone responses were more severely reduced than rod responses, including a patient with visual acuity of 1.0 and 0.8, which is atypical for cone-rod degener-ation.[4] In a similar manner, III-3, the youngest sibling in the present study, had diffuse cone-greater-than-rod dysfunction at a time when the full-field ERG responses were measurable, but he retained a central island of visual acuity, visual field and preserved outer retinal layers in OCT images 13 years later when his symptoms included nyctalopia rather than photophobia or color vision problems. Previous reports have also shown foveal outer retinal preservation on SD-OCT in patients with *FAM161A* mutations and visual acuity between 20/20–20/30.[4] Although the phenotype of patients with retinal degeneration due to *FAM161A* mutations includes both rod and cone dysfunction and degeneration, the retention of visual acuity and a small region of persistent cones near the fovea suggests that foveal cones are preserved until late stages of degeneration in some patients with *FAM161A* mutations, similar to the pattern observed in patients with RD caused by mutations in genes including *ATPase6*, *CDHR1*, *RHO*, and *RDS*.[9,15,16] The current study extends the phenotypic characterization of *FAM161A*-associated arRD by demonstrating that central cones are preserved until late stages of disease progression (Figure 6). The inter-individual variation and preservation of central cones are features which may serve to guide clinicians seeking to identify the molecular cause responsible for arRD in their patients; the central preservation of cones may also provide a useful outcome measure to monitor during disease progression and in response to experimental therapies as they are developed.

Therapeutic interventions aimed at preserving cone structure, either through gene replacement or through neurotrophic factors,[15] might be most beneficial if administered to patients who retain central cones with visual acuity no worse than 20/40. High resolution imaging techniques such as AOSLO may provide a sensitive means of monitoring disease progression and response to experimental therapies in patients with *FAM161A* mutations who retain central visual acuity better than 20/200 and who are able to maintain stable fixation required to permit AOSLO image acquisition, in the absence of high refractive error.

In conclusion, we characterized the retinal phenotype in patients with autosomal recessive RD associated with mutations in *FAM161A* using advanced retinal imaging methodologies. Our findings are consistent with the hypothesis that *FAM161A* is important for normal photoreceptor function and survival, and that the onset and severity of *FAM161A*-associated RD may be affected by environmental or genetic modifiers.[4,5]

Additional studies are needed to understand the factors that modify the phenotype in the siblings of this family. Creation of a mouse model defective in the murine ortholog of *FAM161A* would enable additional assessment of the role this protein plays in retinal structure and survival, could facilitate the search for modifiers that contribute to phenotypic variability, and may expedite the development of therapies such as gene replacement for this severe inherited retinal degeneration.

ACKNOWLEDGMENTS

Dr Ayyagari, the principal investigator and corresponding author, had full access to all the data in the study and takes responsibility for the integrity of the data and the accuracy of the data analysis.

This work was supported by RO1EYO21237 (RA), NIH-P30EY22589 (Department of Ophthalmology, UCSD), NIH-NEI EY002162 (JD), Foundation Fighting Blindness (RA, JD), Research to Prevent Blindness (RA, JD), That Man May See, Inc. (JD), The Bernard A. Newcomb Macular Degeneration Research Fund (JD), Hope for Vision (JD), The Scripps Research Institute (grants DK53505-12 and U54 RR025204 to PL), and The Beutler Foundation (PL).

REFERENCES

1. Cukras C, Gaasterland T, Lee P, et al. Exome analysis identified a novel mutation in the RBP4 gene in a consanguineous pedigree with retinal dystrophy and developmental abnormalities. PLoS One. 2012; 7:e50205. [PubMed: 23189188]
2. Tucker BA, Scheetz TE, Mullins RF, et al. Exome sequencing and analysis of induced pluripotent stem cells identify the cilia-related gene male germ cell-associated kinase (MAK) as a cause of retinitis pigmentosa. Proc Natl Acad Sci USA. 2011; 108:E569–E576. [PubMed: 21825139]
3. Gu S, Kumaramanickavel G, Srikumari CR, et al. Autosomal recessive retinitis pigmentosa locus RP28 maps between D2S1337 and D2S286 on chromosome 2p11-p15 in an Indian family. J Med Genet. 1999; 36:705–707. [PubMed: 10507729]
4. Bandah-Rozenfeld D, Mizrahi-Meissonnier L, Farhy C, et al. Homozygosity mapping reveals null mutations in FAM161A as a cause of autosomal-recessive retinitis pigmentosa. Am J Hum Genet. 2010; 87:382–391. [PubMed: 20705279]
5. Langmann T, Di Gioia SA, Rau I, et al. Nonsense mutations in FAM161A cause RP28-associated recessive retinitis pigmentosa. Am J Hum Genet. 2010; 87:376–381. [PubMed: 20705278]
6. Zobor D, Balousha G, Baumann B, Wissinger B. Homozygosity mapping reveals new nonsense mutation in the FAM161A gene causing autosomal recessive retinitis pigmentosa in a Palestinian family. Mol Vis. 2014; 20:178–182. [PubMed: 24520187]
7. Kumar A, Shetty J, Kumar B, Blanton SH. Confirmation of linkage and refinement of the RP28 locus for autosomal recessive retinitis pigmentosa on chromosome 2p14-p15 in an Indian family. Mol Vis. 2004; 10:399–402. [PubMed: 15215745]
8. Marahnao B, Biswas P, Duncan JL, et al. exomeSuite: Whole exome sequence variant filtering tool for rapid identification of putative disease causing SNVs/indels. Genomics. 2014; 103:169–176. [PubMed: 24603341]
9. Duncan JL, Talcott KE, Ratnam K, et al. Cone structure in retinal degeneration associated with mutations in the peripherin/RDS gene. Invest Ophthalmol Vis Sci. 2011; 52:1557–1566. [PubMed: 21071739]

10. Marmor MF, Fulton AB, Holder GE, et al. ISCEV Standard for full-field clinical electroretinography (2008 update). Doc Ophthalmol. 2009; 118:69–77. [PubMed: 19030905]
11. Duncan JL, Zhang Y, Gandhi J, et al. High-resolution imaging with adaptive optics in patients with inherited retinal degeneration. Invest Ophthalmol Vis Sci. 2007; 48:3283–3291. [PubMed: 17591900]
12. Roorda A, Zhang Y, Duncan JL. High-resolution in vivo imaging of the RPE mosaic in eyes with retinal disease. Invest Ophthalmol Vis Sci. 2007; 48:2297–2303. [PubMed: 17460294]
13. Zach F, Grassmann F, Langmann T, et al. The retinitis pigmentosa 28 protein FAM161A is a novel ciliary protein involved in intermolecular protein interaction and microtubule association. Hum Mol Genet. 2012; 21:4573–4586. [PubMed: 22791751]
14. Di Gioia SA, Letteboer SJ, Kostic C, et al. FAM161A, associated with retinitis pigmentosa, is a component of the cilia-basal body complex and interacts with proteins involved in ciliopathies. Hum Mol Genet. 2012; 21:5174–5184. [PubMed: 22940612]
15. Talcott KE, Ratnam K, Sundquist SM, et al. Longitudinal study of cone photoreceptors during retinal degeneration and in response to ciliary neurotrophic factor treatment. Invest Ophthalmol Vis Sci. 2011; 52:2219–2226. [PubMed: 21087953]
16. Duncan JL, Roorda A, Navani M, et al. Identification of a novel mutation in the CDHR1 gene in a family with recessive retinal degeneration. Arch Ophthalmol. 2012; 130:1301–1308. [PubMed: 23044944]

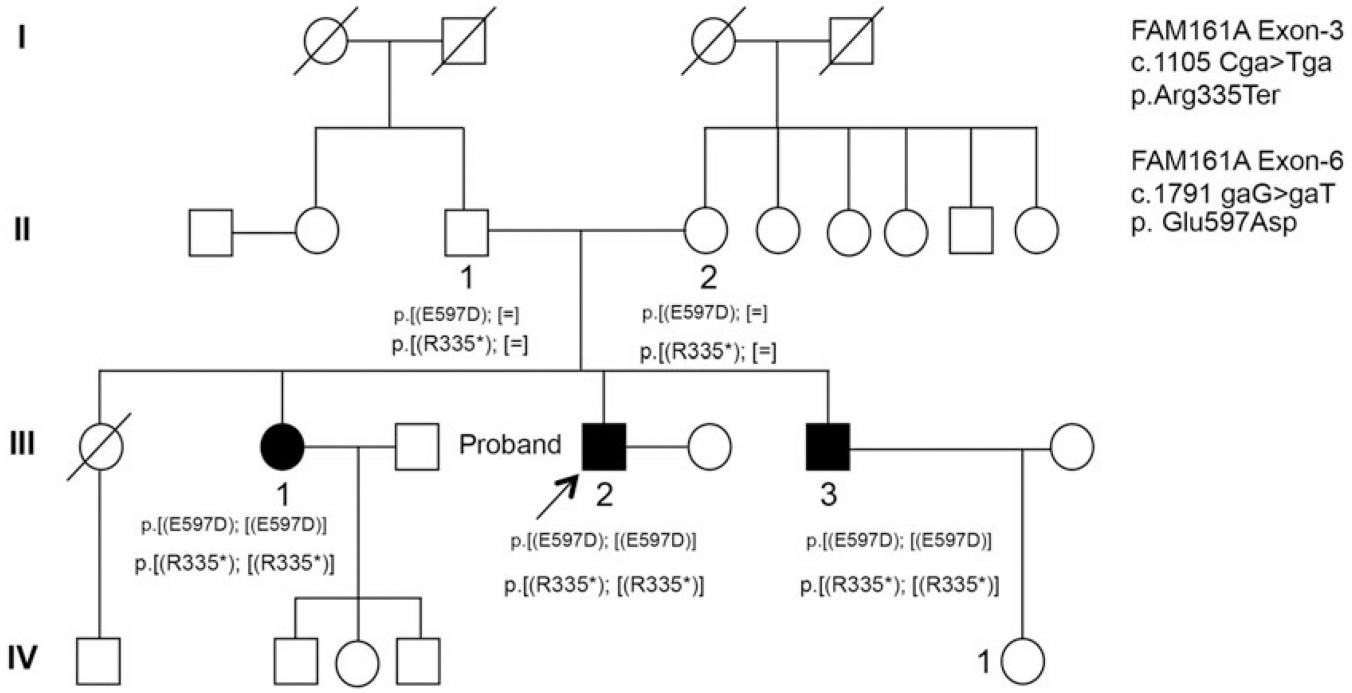

FIGURE 1.

FAM161A mutations segregate with RD. Autosomal recessive retinal degeneration segregates with the c. 1105 C>T and c. 1791 G>T *FAM161A* mutations in a pedigree of Indian origin. Squares indicate males; circles, females; shaded symbols, retinal degeneration; slash marks, deceased individuals.

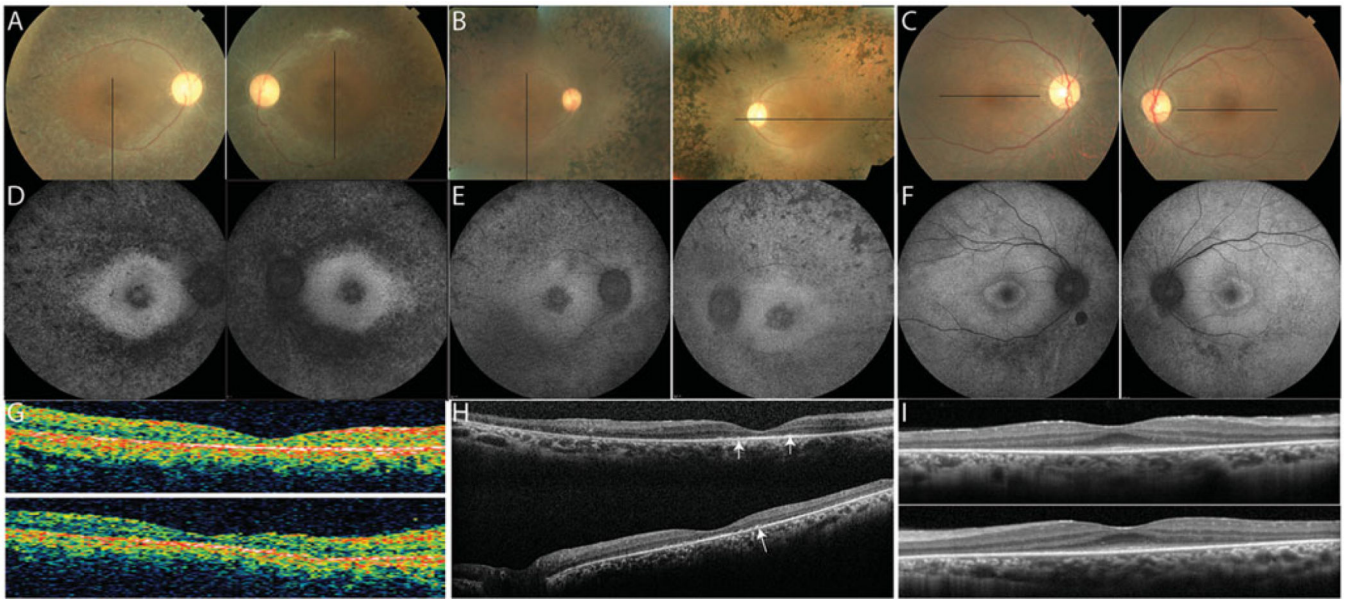

FIGURE 2.

Clinical features at the time of most recent examination in the affected members. (A–C) color fundus photos; (D–F) fundus autofluorescence; (G–I) optical coherence tomography scans of the right (top) and left (bottom) eyes. Black lines on color photos indicate location of OCT scans. Homozygotes show increased autofluorescence around the fovea and severe outer retinal layer loss; spectral-domain OCT shows hyper-reflective profiles in the subretinal space (Figure 2H, white arrows).

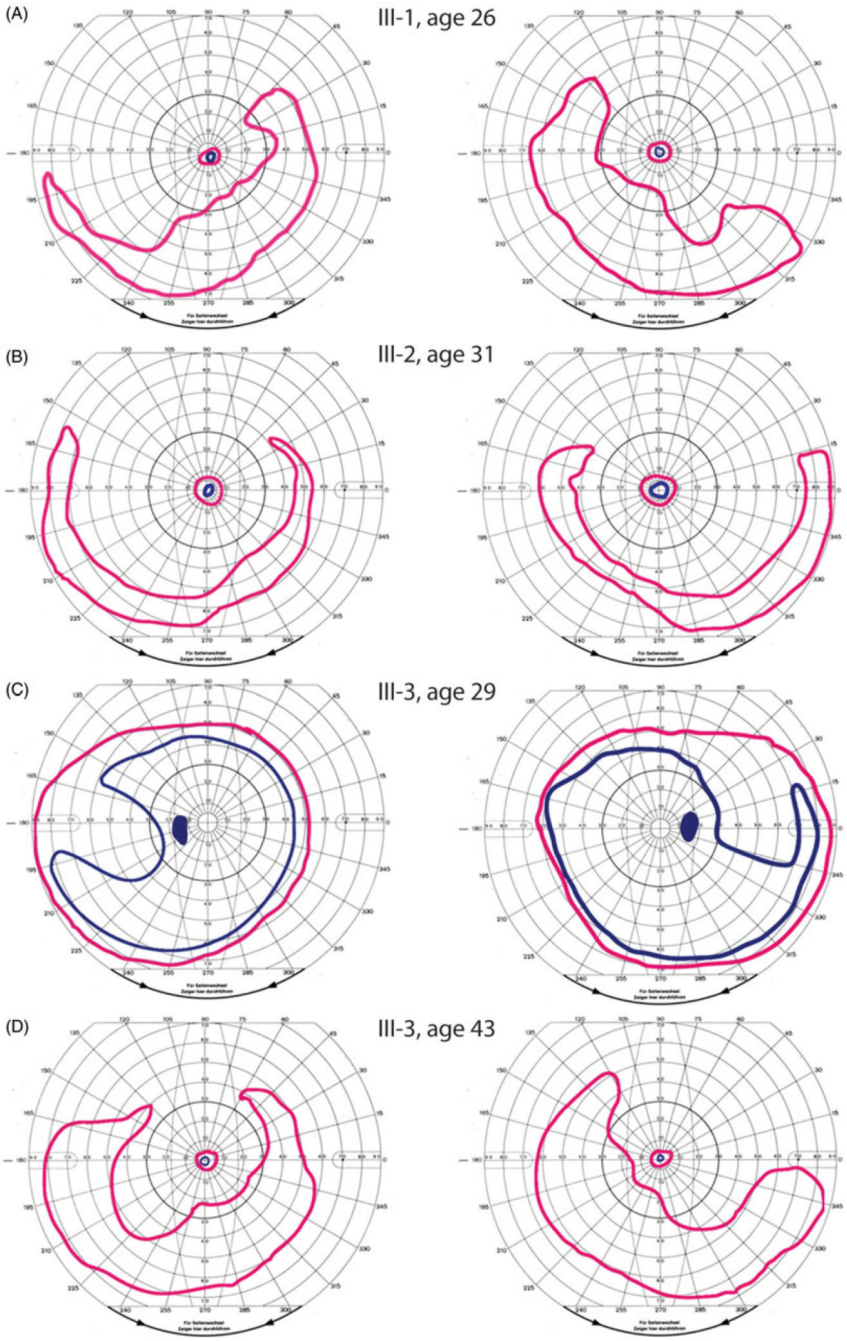

FIGURE 3.

Visual fields in *FAM161A*-associated RD demonstrate a range of disease onset and severity. Goldmann kinetic perimetry at earliest examination in the affected family members shows small central islands with preserved inferotemporal crescents in III-1, age 26, and III-2, age 31 (Figure 3A and B), with superotemporal scotomas present at early stages (III-3, age 29, figure 3C). At ages 47 and 44, vision was reduced to light perception in III-1 and III-2, while III-3 retained a central island with a preserved inferotemporal crescent similar to the pattern observed at diagnosis 10–15 years earlier in his siblings (Figure 3D). Left panels

show left visual fields while right panels show right visual fields. Pink peripheral isopters show responses to a V4e target for all subjects except III-1, for whom the largest target tested was IV4e; blue central isopters show responses to a I4e target for all subjects.

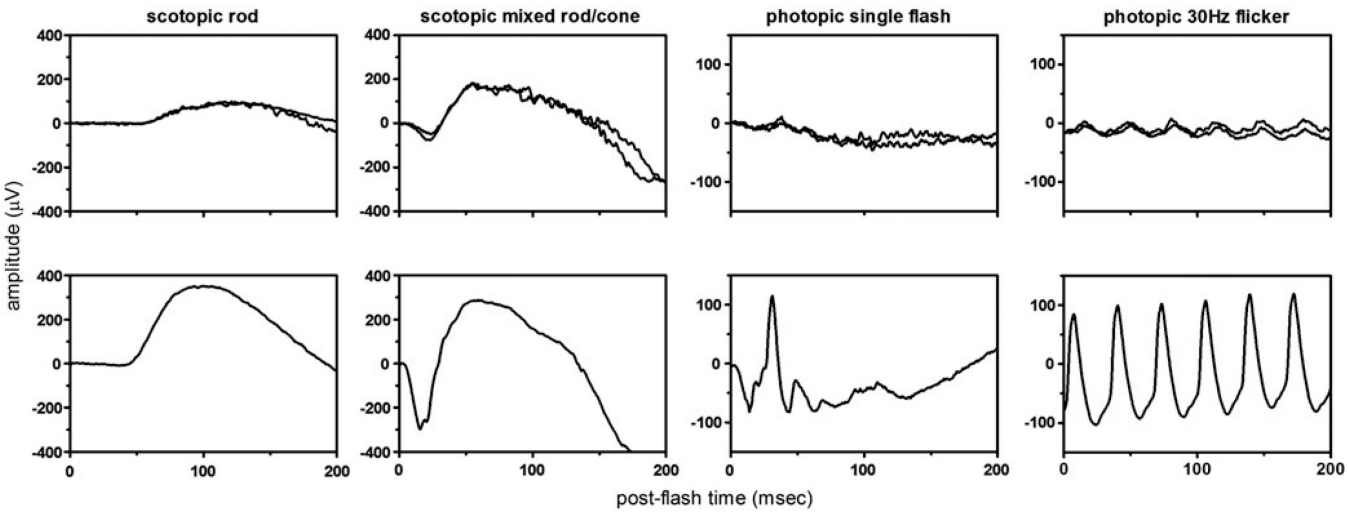

FIGURE 4.

Retinal dysfunction in *FAM161A*-related RD. Full-field ISCEV standard ERGs from both eyes of III-3 recorded at age 29 compared with an age matched control (bottom row) showed moderate reduction of scotopic amplitudes, severe reduction of photopic amplitudes, and delayed timing of photopic responses in both eyes of III-3 compared to normal. Full-field ERG responses were not measurable to any stimuli at the earliest dates they were performed in patients III-1 and III-2 (Table 1).

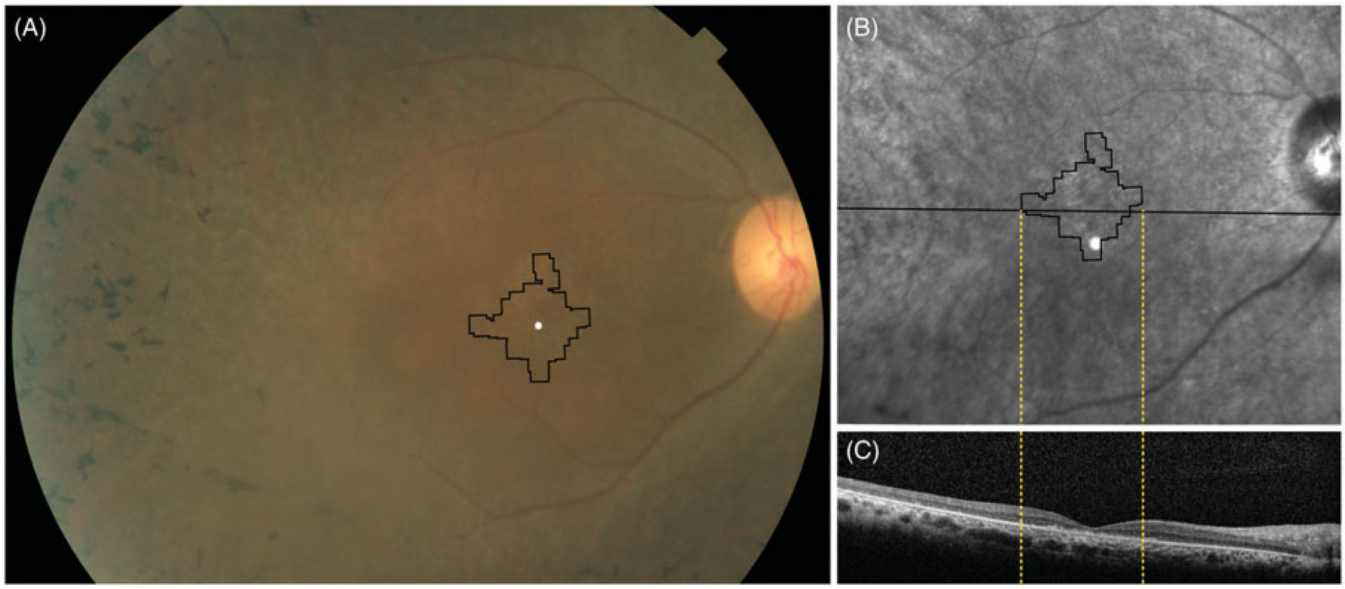

FIGURE 5.

Clinical images of *FAM161A*-related RD. (A) Color fundus photograph showing bone spicule pigmentary changes anterior to the arcades, retinal vascular attenuation and mild disc pallor with black lines outlining the retinal region imaged using AOSLO. (B) Infrared fundus photograph showing RPE irregularity within the arcades; thin black lines outline the region imaged using AOSLO, while thick black line indicates SD-OCT location. (C) SDOCT through the anatomic fovea shows a thin outer nuclear layer extending a few degrees from the anatomic fovea. Black rectangle indicates extent of magnified inset shown in Figure 6(B).

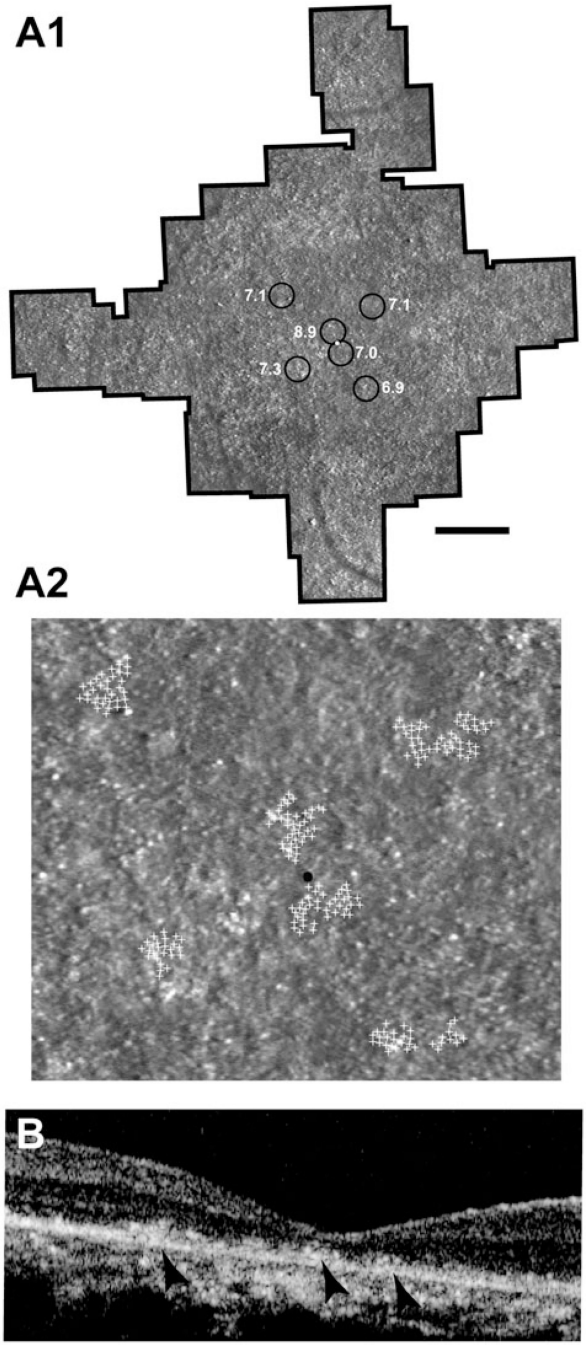

FIGURE 6.

High-resolution foveal images of III-2 acquired using adaptive optics scanning laser ophthalmoscopy (AOSLO). (A1) Cones are not seen clearly throughout most of the montage, but where quantifiable cones are visible, cone spacing is increased by 6.9–8.9 standard deviations above the normal mean (circles: standard deviations from normal mean). White circle indicates the anatomic fovea. (A2) shows location of cones identified for quantification with white + symbols; black circle indicates the anatomic fovea. (B) Horizontal foveal SDOCT shows a thin external limiting membrane where cones are seen

centrally with hyper-reflective lesions in the outer retinal layers (arrows) beneath the fovea and peripheral to the locations where cones are seen (scale bar = 1°).

TABLE 1

Clinical and molecular characteristics of affected and unaffected family members studied.

Patient no. /sex	Age at visit (Y)	Age at first symptoms (Y)	Age at diagnosis (Y)	Nucleotide change at c.1105 C>T	Zygosity	Nucleotide change at c.1791G>T	Zygosity	Visual acuity at diagnosis OD/OS	Refraction OD, OS	Goldmann Visual Field (V4e) at diagnosis	Full-field ERG at diagnosis
II-1/M	72	n/a	n/a	C/T	Heterozygous	G/T	Heterozygous	20/25, 20/25	Piano, piano	NP, NP	NP, NP
II-2/F	67	n/a	n/a	C/T	Heterozygous	G/T	Heterozygous	20/20, 20/20	Piano, piano	NP, NP	NP, NP
III-1/F	47	19	24	T/T	Homozygous	T/T	Homozygous	20/40-1, 20/60-2	−2.00 + 3.25 × 094, −2.00 + 3.25 × 083	Central 10° island with inferotemporal crescent OU (IV4e)	Not measurable to all stimuli OU
III-2/M	44	19	27	T/T	Homozygous	T/T	Homozygous	20/25-1, 20/32-1	−3.50 + 1.75 × 110, −3.75 + 1.75 × 060	Central 15° island with inferotemporal crescent OU	Not measurable to all stimuli OU
III-3/M	43	42	29	T/T	Homozygous	T/T	Homozygous	20/25 + 2, 20/25 + 1	−8.75 + 3.50 × 105, −8.75 + 3.25 × 075	Full OU; Midperipheral scotoma temporally to I4e OU	Cone greater than rod dysfunction OU

Y, years; OD, right eye; OS, left eye; OU, both eyes; M, male; F, female; n/a, not applicable; NP, not performed.

Visual acuity represents best spectacle-corrected acuity.